eLIFE
elifesciences.org

Figures and figure supplements

Drep-2 is a novel synaptic protein important for learning and memory

Till F M Andlauer, et al.

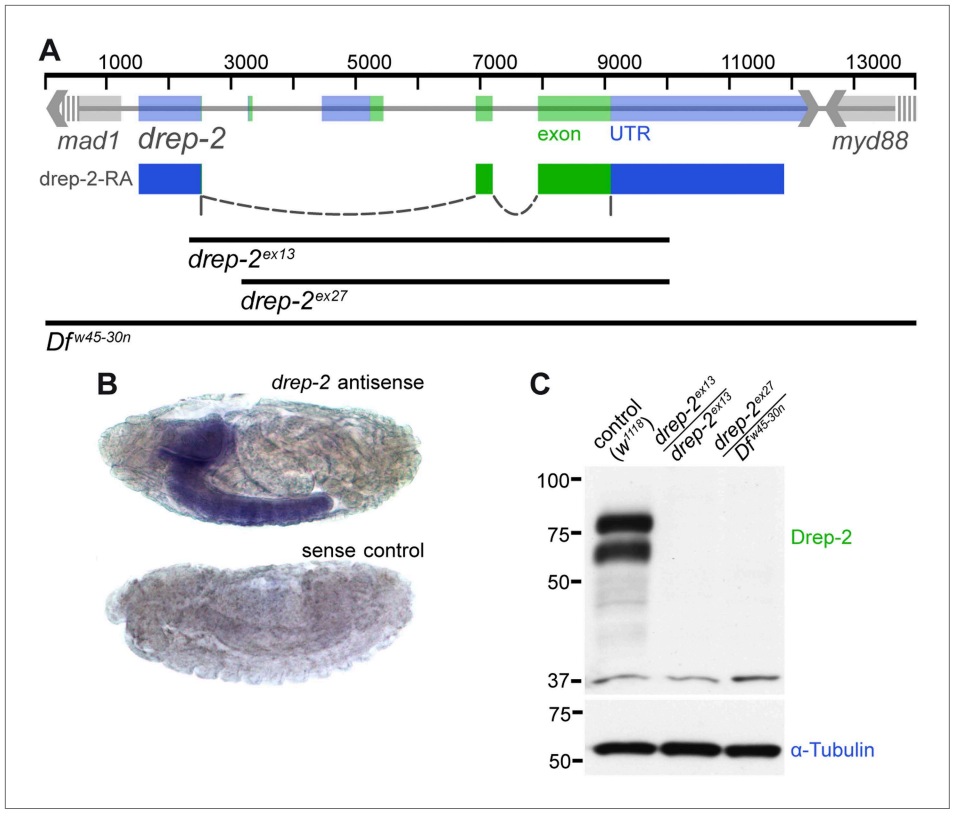

Figure 1. Expression and mutants of *drep-2*. (**A**) Genetic scheme of the *drep-2* locus on chromosome IIR. The neighboring genes *mad-1* and *myd88* extend beyond the sequence displayed. The cDNA labeled *drep-2-RA* was used for rescue experiments. Blue: untranslated regions; green: exons; black lines: deleted regions in the mutants. (**B**) In situ hybridization of *drep-2* reveals a neuronal expression pattern (stage 17). (**C**) Western blot of adult fly head extracts using the anti-Drep-2$^{C\text{-}Term}$ antibody. Drep-2 isoforms are predicted to run at 52 and 58 kDa. The signal is absent in both the *drep-2*^{ex13} and the *drep-2*^{ex27}/*Df*$^{w45\text{-}30n}$ mutant.

DOI: 10.7554/eLife.03895.003

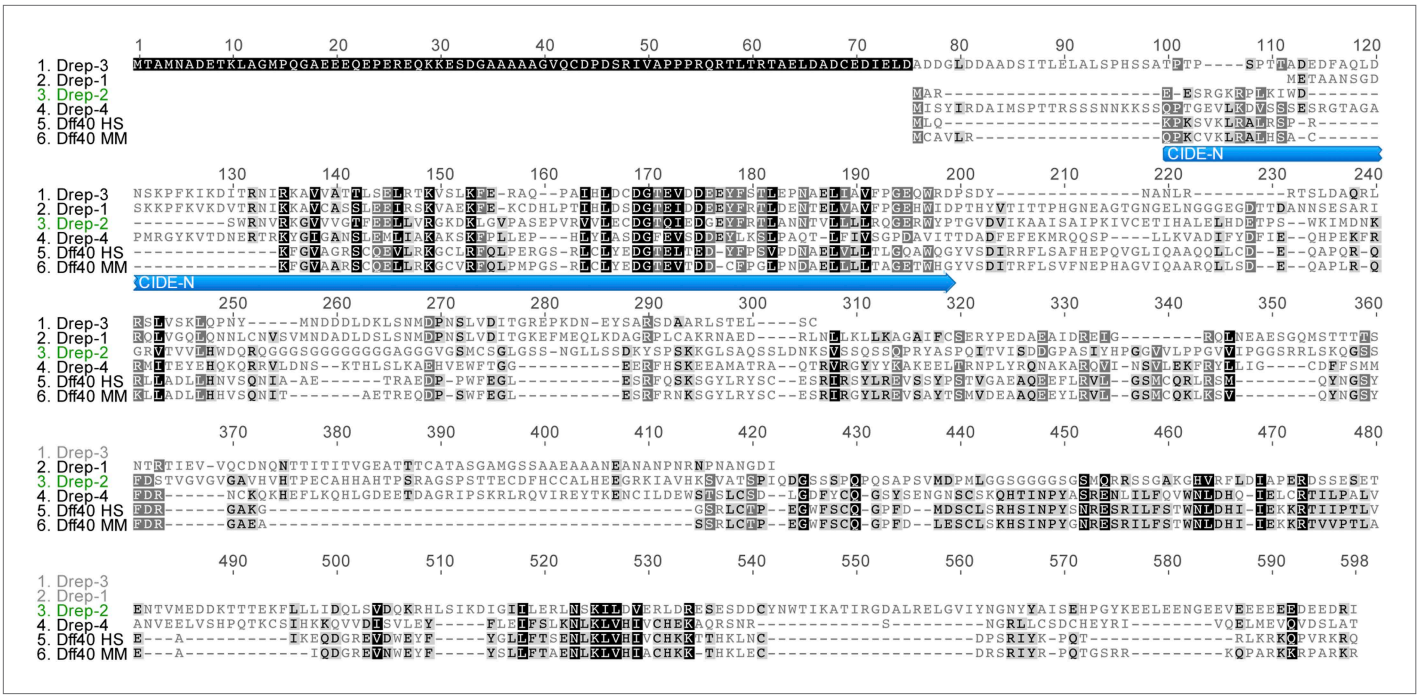

Figure 1—figure supplement 1. Drep protein alignment. Sequence alignment of all four Drosophila Dff proteins, as well as human (HS) and murine (MM) Dff40. Drep-4 has the strongest similarity to Dff40, yet Drep-2 also shows conserved motifs in addition to the CIDE-N domain. The alignment was created using Geneious v5.3.6. (http://www.geneious.com)

DOI: 10.7554/eLife.03895.004

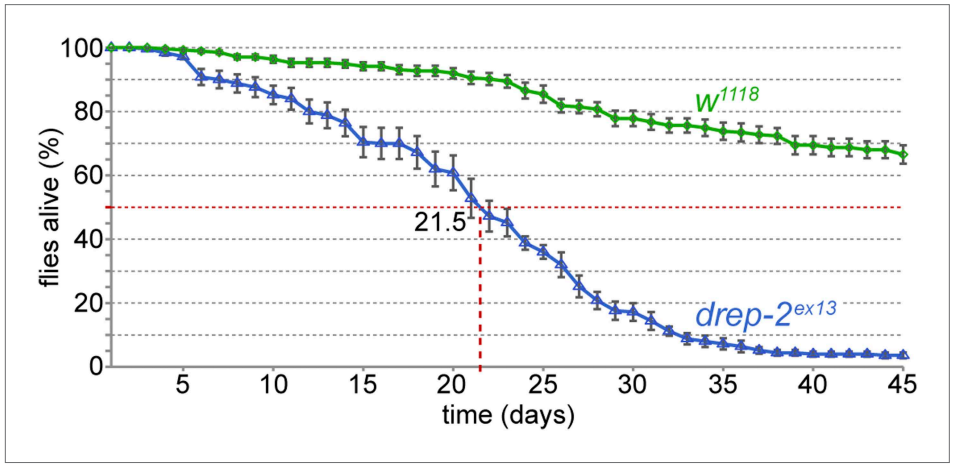

Figure 1—figure supplement 2. Reduced lifespan of *drep-2*^{ex13} mutants. Comparison to isogenic *w*^{1118} control flies: 50% of mutant flies were dead after 21.5 days. Mutant: n = 10 vials (each containing 25 flies), control: n = 11.

DOI: 10.7554/eLife.03895.005

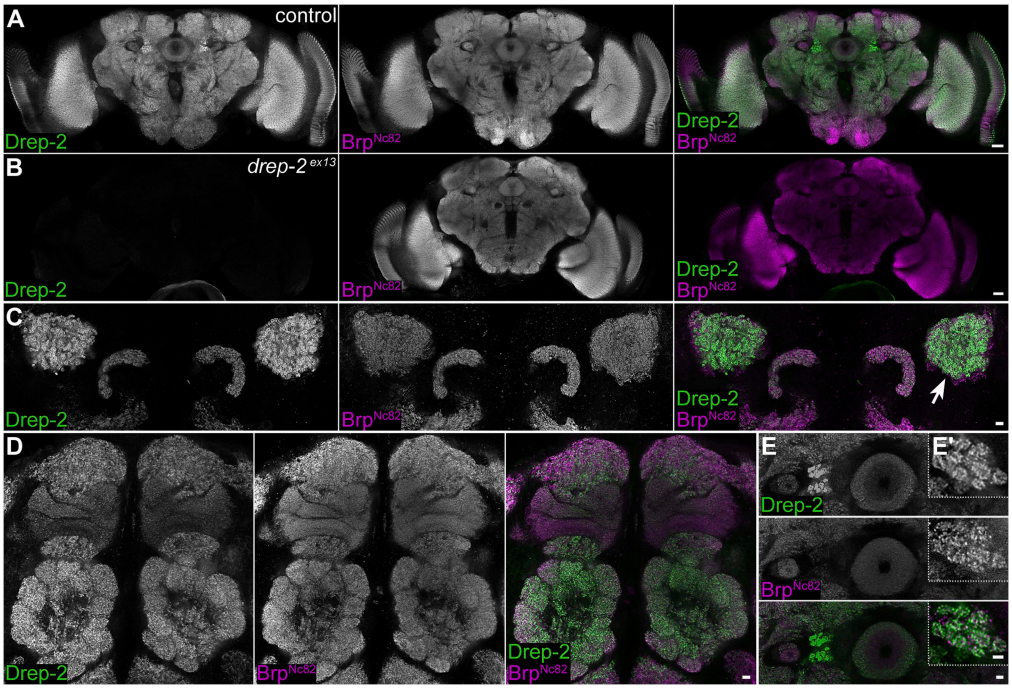

Figure 2. Synaptic Drep-2 staining in the CNS. (**A**–**B**) Confocal frontal sections of adult *Drosophila* brains. Anti-Drep-2$^{C\text{-}Term}$ and Brp^{Nc82} immunostaining; the latter marks all synaptic active zones. Synaptic Drep-2$^{C\text{-}Term}$ signal is visible throughout the brain of wild-type flies (**A**). Complete loss of the anti-Drep-2$^{C\text{-}Term}$ staining can be observed in *drep-2*^{ex13} mutants (**B**). Scale bars: 20 μm. (**C**–**E**) Frontal sections of wild-type brains, anti-Drep-2$^{C\text{-}Term}$, and Brp^{Nc82} staining. Scale bars: 5 μm. (**C**) Posterior–dorsal detail showing strong Drep-2 staining in MB calyces (arrow). (**D**) Anterior frontal section with antennal lobes and MB lobes. (**E**) Ellipsoid body in the central complex and bulbs (lateral triangles) (**E′**: magnification of strong Drep-2 staining in bulbs).

DOI: 10.7554/eLife.03895.006

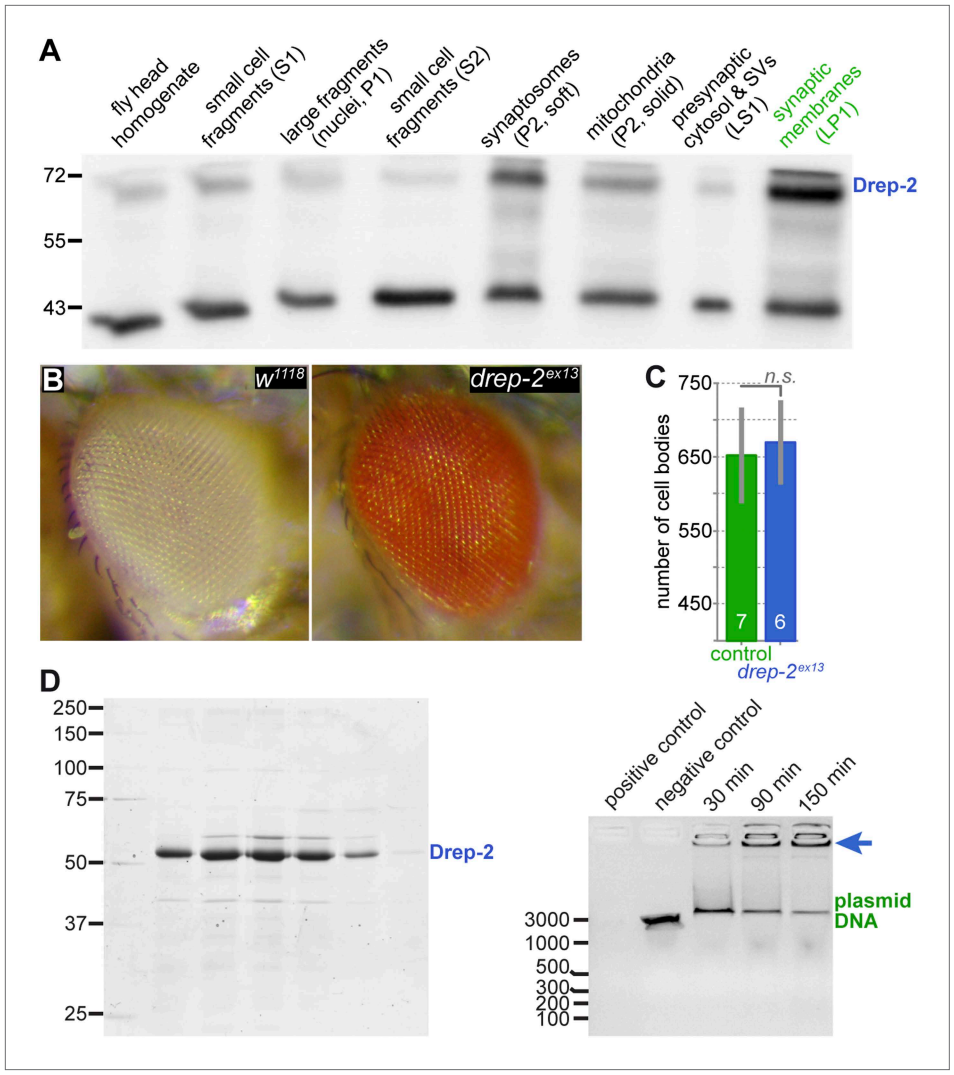

Figure 3. No evidence for a role of Drep-2 in regulation of apoptosis. (**A**) Synaptosome-like preparation of adult wild-type head extracts (***Depner et al., 2014***), probed with Drep-2$^{C\text{-}Term}$. Drep-2 is concentrated in fractions containing synaptic membranes. S = supernatant, P = pellet, L = (after) lysis. Please see the protocol by ***Depner et al. (2014)*** for a more detailed explanation of the fractionation procedure. (**B**) Mutants (*drep-2*^{ex13}) did not show a rough eye phenotype. The facet eyes of flies, highly ordered structures, are often affected in apoptosis mutants. By contrast, the eyes of *drep-2* mutants appeared normal. (**C**) The number of mb247-positive KCs does not differ between *drep-2*^{ex13} mutants and controls. GFP was expressed using the MB KC driver mb247-Gal4. GFP-positive cell bodies were counted and compared between genotypes. No significant difference was found between mean cell body counts (Mann–Whitney U test, $p = 0.886$). Average cell body counts were in the expected range: control = 651, mutant = 669, published = 700 (***Schwaerzel et al., 2002***). (**D**) Purified Drep-2 does not degrade linearized plasmid DNA. Left: SDS-PAGE of the final elusion profile of purified Drep-2, loaded onto a HighLoad Superdex S200 16/60 column. Right: Nuclease activity assay of purified Drep-2 analyzed by 1% (wt/vol) agarose gel. Drep-2 was incubated in a time course experiment with linearized plasmid DNA. No nuclease activity could be detected. Instead, Drep-2 seemed to precipitate DNA, as evidenced by high-molecular DNA not entering into the agarose gel when incubated with Drep-2 (arrow).

DOI: 10.7554/eLife.03895.007

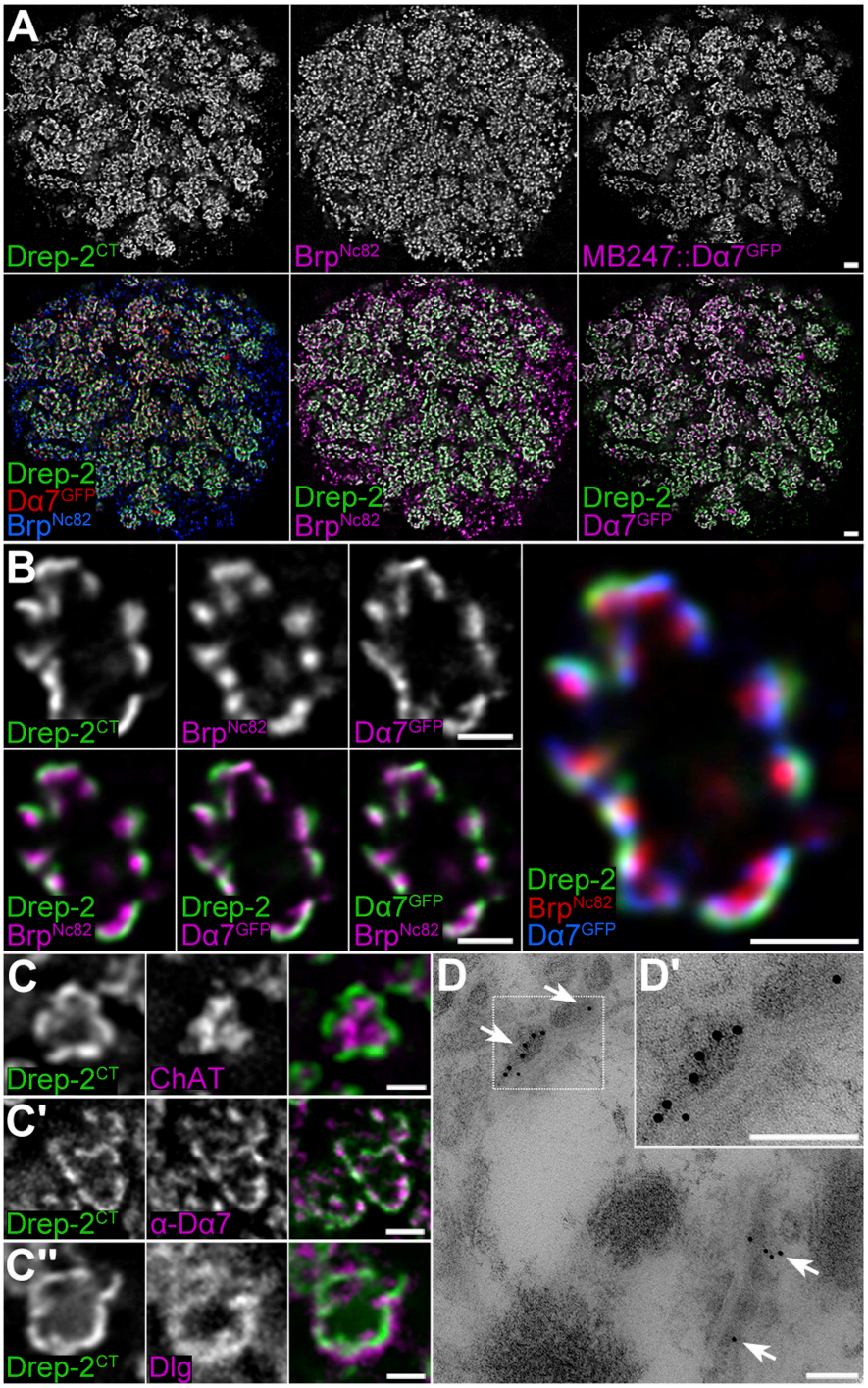

Figure 4. Drep-2 is enriched at KC postsynapses. (**A**–**B**) Drep-2$^{C\text{-}Term}$ and Brp^{Nc82} staining in animals expressing the construct mb247::Dα7^{GFP} that marks acetylcholine receptors in MB KCs. (**A**) Detailed image of the MB calyx. Scale bar: 2 μm. (**B**) Detail of a single microglomerulus in the calyx. Drep-2$^{C\text{-}Term}$ overlaps with postsynaptic mb247::Dα7^{GFP} and not with presynaptic Brp. Scale bars: 1 μm. (**C**) Localization of Drep-2 relative to choline acetyltransferase (ChAT, presynaptic cytosol, C), the postsynaptic ACh receptor subunit Dα7 (antibody staining, **C′**), and the postsynaptic scaffolding protein Discs large (Dlg, **C″**). Drep-2 colocalizes with postsynaptic markers. Scale bars: 1 μm. (**D**) Post-embedding immunoelectron microscopy of Drep-2$^{C\text{-}Term}$ in the calyx. Arrows: Clusters of postsynaptic Drep-2$^{C\text{-}Term}$. Scale bars: 100 nm.

DOI: 10.7554/eLife.03895.008

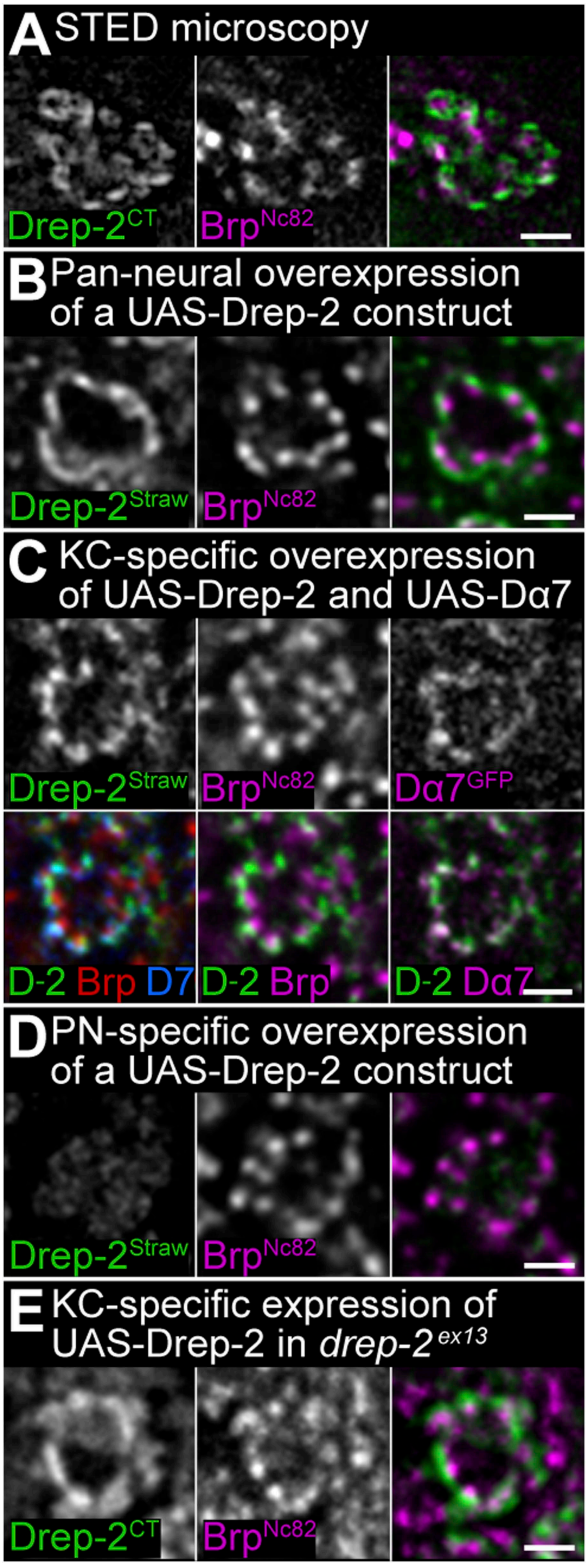

Figure 4—figure supplement 1. Drep-2 localizes to postsynaptic membranes of KCs in the calyx. (**A**) STED microscopy superresolution recording of Drep-2$^{C\text{-}Term}$; the Brp^{Nc82} channel is in normal

Figure 4—figure supplement 1 Continued on next page

Figure 4—figure supplement 1 Continued
confocal mode. The Drep-2 signal does not overlap with presynaptic Brp. Scale bar: 1 μm. (**B**–**E**) Expression of *drep-2* constructs in KCs yields a label resembling the Drep-2 antibody staining. Comparison to Brp^{Nc82}; all scale bars: 1 μm. (**B**) Pan-neural overexpression. $Elav^{c155}$-Gal4 and UAS-Drep-$2^{mStrawberry}$; mStrawberry signal is shown. (**C**) KC-specific overexpression. C305a-Gal4, UAS-Drep-$2^{mStrawberry}$, and UAS-Dα7^{GFP}; mStrawberry and GFP signals are shown. D-2 = Drep-$2^{mStrawberry}$, D7 = Dα7^{GFP}. (**D**) PN-specific overexpression. Gh146-Gal4 and UAS-Drep-$2^{mStrawberry}$; diffuse mStrawberry is shown. (**E**) KC-specific expression of UAS-Drep-2 in the *drep-2*^{ex13}-mutant background. Mb247-Gal4 and untagged UAS-Drep-2; Drep-$2^{C\text{-}Term}$ staining is shown.
DOI: 10.7554/eLife.03895.009

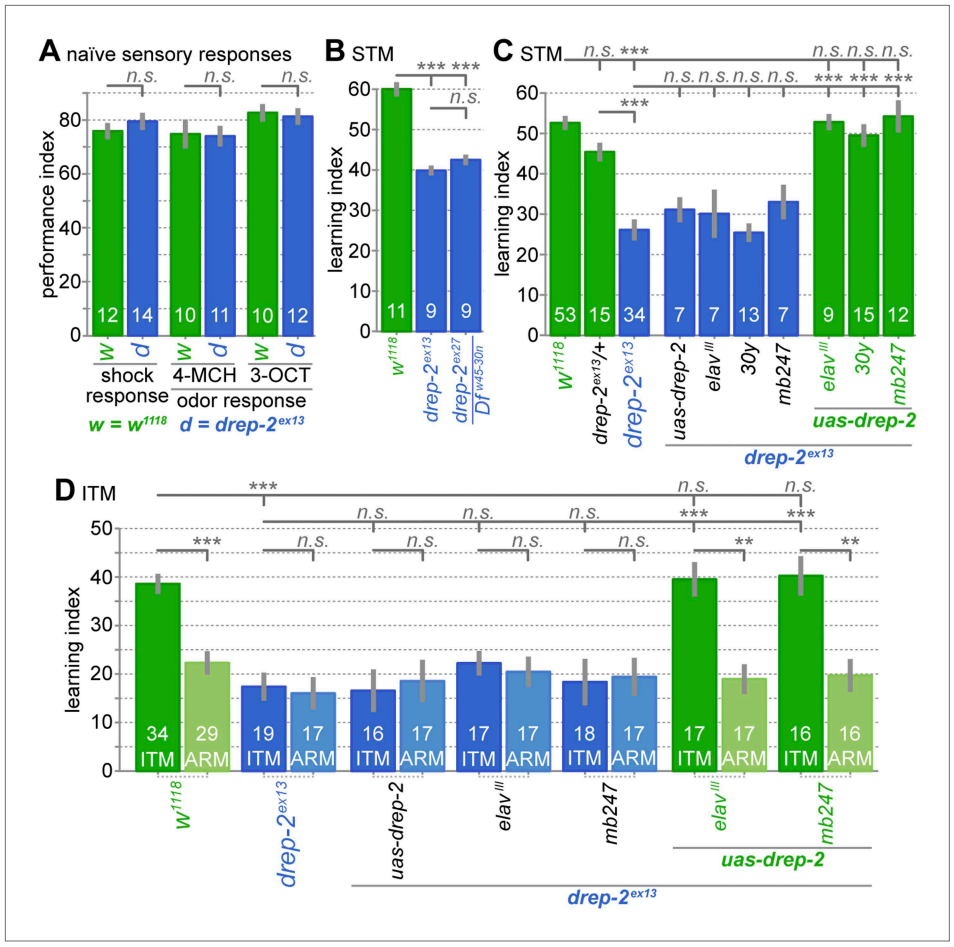

Figure 5. Drep-2 is required in KCs for olfactory short- and intermediate-term memory. (**A**) Flies mutant for *drep-2* sense electric shock and the odors 4-methyl-cyclohexanol (4-MCH) and 3-octanol (3-OCT) normally; there is no difference in mean performance indices between mutants and isogenic w^{1118} control flies (Mann–Whitney U tests (MWU)). Sample sizes n are indicated with white numbers; grey bars show SEMs. (**B**) Both mutants *drep-2*^{ex13} and *drep-2*^{ex27}/*Df*$^{w45\text{-}30n}$ are deficient in aversive olfactory conditioning, 3 min STM in a T-maze. The graph shows mean learning indices and SEMs. Mutants performed significantly worse than isogenic controls (MWU: $p = 0.00001$ for both comparisons, Bonferroni-corrected significance level $\alpha = 0.0167$, 3 tests). (**C**) Re-expression of *drep-2* cDNA with elav^{III}-Gal4 (pan-neural), 30y-Gal4 (MB KCs), or mb247-Gal4 (MB KCs) restores the deficit to normal levels. Heterozygous *drep-2*^{ex13} mutants do not display a significant deficit. MWU for individual comparisons showed a significant difference between these groups ($\alpha = 0.0042$, 12 tests): w^{1118} and *drep-2*^{ex13} ($p < 0.00001$), *drep-2*^{ex13}/*drep-2*^{ex13} and *drep-2*^{ex13}/+ ($p < 0.00001$), *drep-2*^{ex13} and *drep-2*^{ex13};*uas-drep-2/elav*^{III}*-gal4* ($p < 0.00001$), *drep-2*^{ex13} and *drep-2*^{ex13};*uas-drep-2/30y-gal4* ($p < 0.00001$), *drep-2*^{ex13} and *drep-2*^{ex13};*uas-drep-2/mb247-gal4* ($p < 0.00001$). None of the differences indicated as not significant had a $p < 0.12$, except for w^{1118} and *drep-2*^{ex13}/+ ($p = 0.03851$; not significant in the case of $\alpha = 0.0042$). (**D**) Intermediate-term memory (ITM = ASM + ARM) performance. Mutants (*drep-2*^{ex13}) are defective in ASM, but not in ARM. The defect can be restored with elav^{III}-Gal4 or mb247-Gal4 (30y-Gal4 was not used here). Statistical tests were run separately for ITM and ARM. For ITM, MWU for individual comparisons showed a significant difference between these groups ($\alpha = 0.00625$, 8 tests): w^{1118} and *drep-2*^{ex13} ($p < 0.0001$), *drep-2*^{ex13} and *drep-2*^{ex13};*uas-drep-2/elav*^{III}*-gal4* ($p < 0.0001$), *drep-2*^{ex13} and *drep-2*^{ex13};*uas-drep-2/mb247-gal4* ($p < 0.0001$). For assessing differences in ARM, ITM and ARM performances of each genotype were compared with MWU. The following genotypes showed a significant difference between ITM and ARM ($\alpha = 0.0071$, 7 tests): w^{1118} ($p < 0.0001$), *drep-2*^{ex13};*uas-drep-2/elav*^{III}*-gal4* ($p = 0.0002$), *drep-2*^{ex13};*uas-drep-2/mb247-gal4* ($p = 0.0006$). None of the differences indicated as not significant had a $p < 0.11$.

DOI: 10.7554/eLife.03895.010

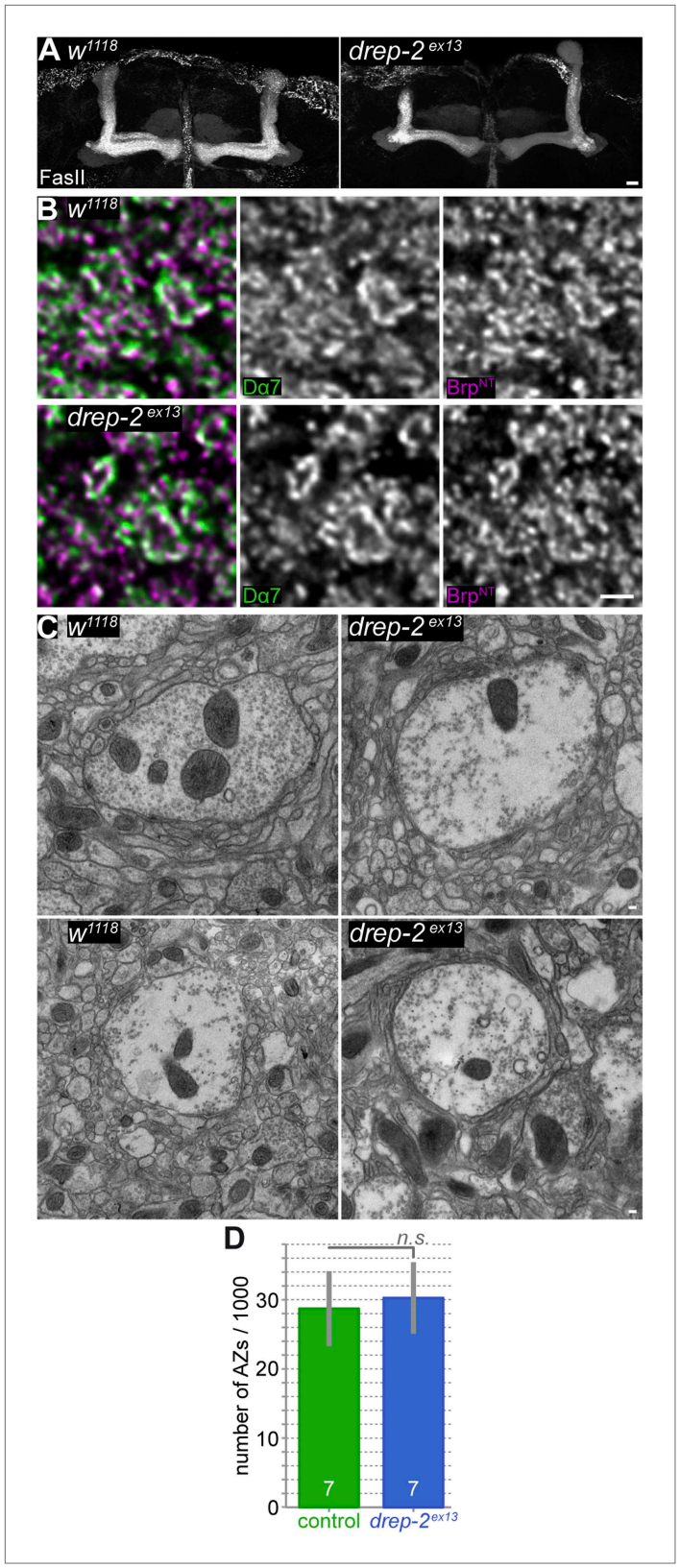

Figure 5—figure supplement 1. PN-KC synapses appear morphologically normal in *drep-2* mutants. (**A**) Absence of major neuroanatomical defects in *drep-2*^{ex13} mutant brains. MB lobes, Fasciclin II (FasII) staining,

Figure 5—figure supplement 1 Continued on next page

Figure 5—figure supplement 1 Continued
maximum intensity projections. Scale bar: 10 μm. (**B**) Antibody staining of w^{1118} control and *drep-2*^{ex13} mutant brains, using antibodies against the postsynaptic ACh receptor subunit Dα7 and presynaptic Brp^{N-Term}. Focus on microglomeruli of PN-KC synapses in the MB calyx. Microglomeruli of mutants appear structurally normal. Scale bar: 1 μm. (**C**) Electron microscopy of w^{1118} control and *drep-2*^{ex13} mutant brains. Microglomeruli and postsynaptic KC profiles of mutants appear structurally normal. Scale bars: 100 nm. (**D**) The number of synapses (active zones) in the MB calyx does not significantly differ between *drep-2*^{ex13} mutants and w^{1118} controls. Syd-1-positive spots were counted and compared between genotypes as described (***Kremer et al., 2010***). No significant difference was found between the number of spots (MWU, $p = 0.62$). Average synapse counts were in the range expected (28,000–30,000 [***Kremer et al., 2010***]).
DOI: 10.7554/eLife.03895.011

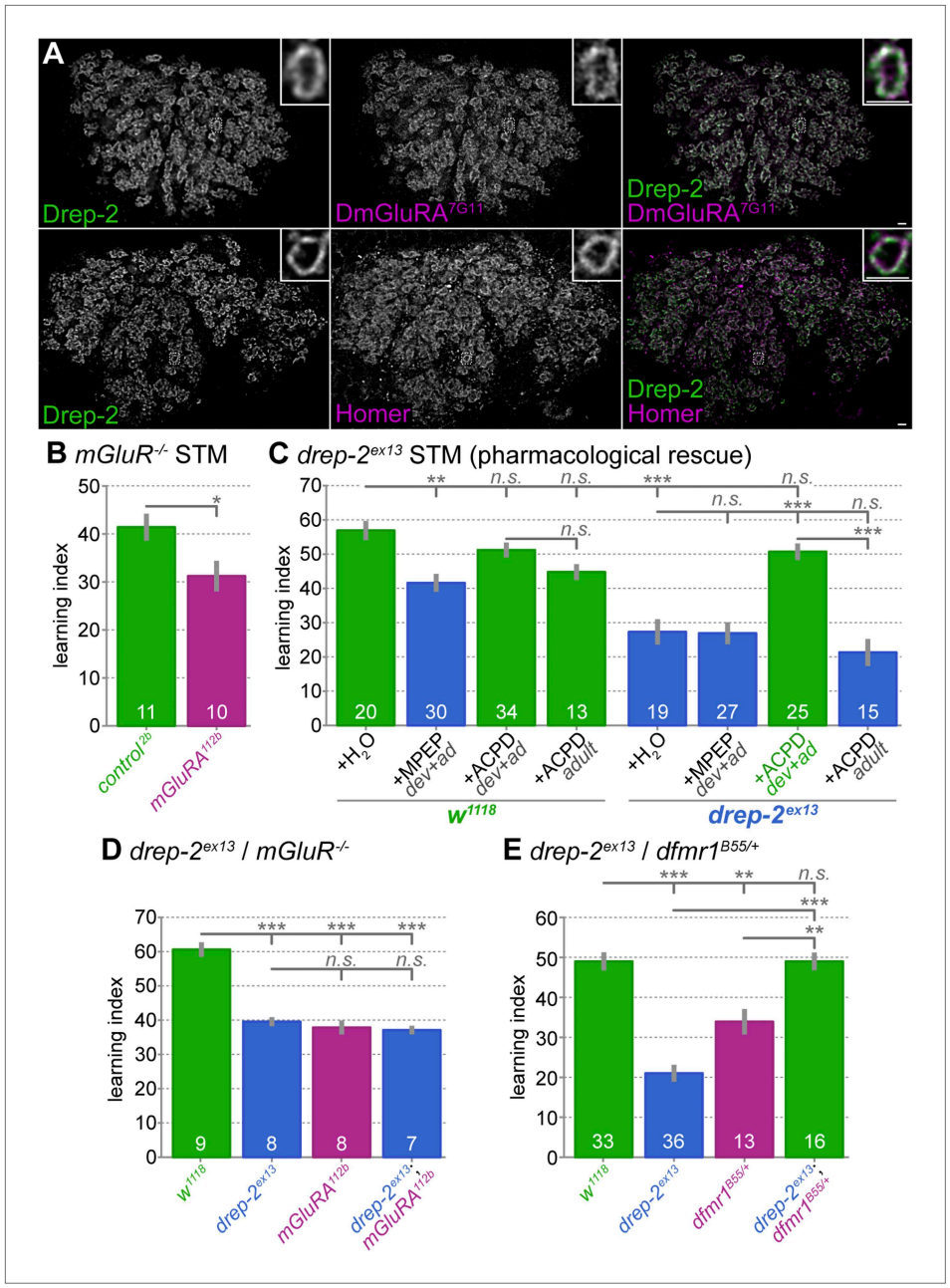

Figure 6. Functional overlap between Drep-2 and mGluR in olfactory conditioning. (**A**) Wildtype adult MB calyces stained with Drep-2$^{C\text{-}Term}$ and DmGluRA^{7G11} (first row) or with Drep-2$^{C\text{-}Term}$ and anti-Homer (second row). Drep-2 colocalizes tightly with both proteins. The insets show single microglomeruli. Scale bars: 2 μm. (**B**) Flies carrying the mutation *dmGluRA*^{112b} are deficient in aversive olfactory conditioning STM when compared to isogenic *dmGluRA*^{2b} controls that do express DmGluRA; MWU: p = 0.043, α = 0.05. The graph shows mean learning indices and SEMs; sample sizes n are indicated with white numbers. (**C**) The *drep-2*^{ex13} phenotype in olfactory STM can be rescued by raising animals on food containing the DmGluRA agonist 1S,3R-ACPD (ACPD). Food was supplemented throughout development and adulthood with either the DmGluRA receptor antagonist MPEP (9.7 μM) or the agonist ACPD (72.2 μM) diluted in H_2O (label: *dev+ad*). Control animals received only H_2O. One group of animals was transferred to food supplemented by ACPD only after eclosion and not during development; the corresponding experiments are indicated by the label *+ACPD adult*. MPEP lowered the *w*^{1118} performance significantly (MWU p = 0.0003). MPEP did not alter *drep-2*^{ex13} indices (p = 0.8772) and ACPD did not change *w*^{1118} performance (p = 0.1145). ACPD rescued the *drep-2* mutant phenotype to control levels if fed during both development and adulthood (comparison of *drep-2*^{ex13} *+ACPD dev+ad* to untreated *drep-2*^{ex13}: p < 0.00001; comparison to untreated *w*^{1118}: p = 0.0945). ACPD

Figure 6. Continued on next page

Figure 6. Continued

did not rescue the mutant phenotype if fed only during adulthood (*+ACPD adult*, no significant difference to untreated *drep-2*^{ex13} ($p = 0.2281$), significant difference to mutants treated with ACPD during both development and adulthood ($p < 0.00001$)). The difference between untreated *w*^{1118} and *drep-2*^{ex13} flies was also significant ($p < 0.00001$). Significance level $\alpha = 0.005$ (10 tests). (**D**) Phenotypes of *drep-2*^{ex13}; *dmGluRA*^{112b} double mutants were non-additive. Both *drep-2*^{ex13} and *dmGluRA*^{112b} single mutants showed significantly lower olfactory STM than isogenic controls (MWU, $p = 0.00008$ for both comparisons). Double mutants showed similar learning indices (comparison to *w*^{1118}: $p = 0.00018$). The two single mutants and the double mutant did not significantly differ from each other ($p > 0.178$). $\alpha = 0.0083$ (6 tests). (**E**) Loss of *drep-2* antagonizes *dfmr1* phenotypes in olfactory conditioning STM. Both homozygous *drep-2*^{ex13} mutants and heterozygous *dfmr1*^{B55}/+ mutants are deficient in olfactory learning STM, but double mutants carrying both alleles do learn. The graph shows mean learning indices and SEMs. MWU for individual comparisons ($\alpha = 0.01$, 5 tests): *w*^{1118} and *drep-2*^{ex13} $p < 0.00001$, *w*^{1118} and *dfmr1*^{B55}/+ $p = 0.00069$, *w*^{1118} and *drep-2*^{ex13}; *dfmr1*^{B55}/+ $p = 0.83751$, *drep-2*^{ex13} and *drep-2*^{ex13}; *dfmr1*^{B55}/+ $p < 0.00001$, *dfmr1*^{B55}/+ and *drep-2*^{ex13}; *dfmr1*^{B55}/+ $p = 0.00071$.

DOI: 10.7554/eLife.03895.012

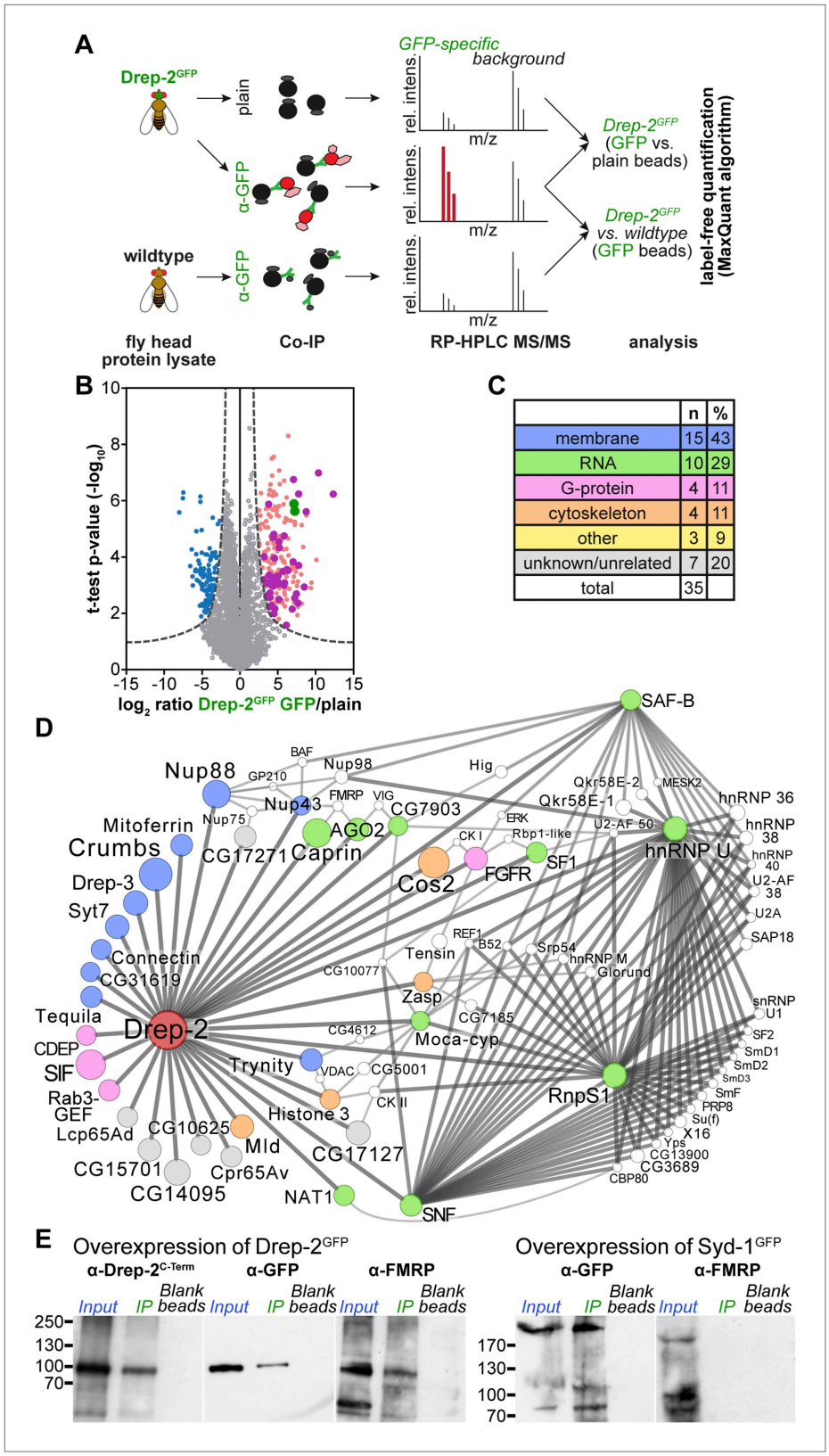

Figure 7. Quantitative mass spectrometry: Drep-2 and FMRP were found in a common protein complex. (**A**) Strategy for the identification of Drep-2 interactors by quantitative mass spectrometry. UAS-Drep-2^{GFP} was overexpressed using the pan-neural driver line elav^{c155}-Gal4. (**B**) Volcano plot showing proteins from Drep-2^{GFP} flies

Figure 7. Continued on next page

Figure 7. Continued

binding to anti-GFP and/or plain control beads. A hyperbolic curve (set at an FDR of 1%) separates GFP-enriched proteins (light pink) from background (grey). Proteins enriched in the control are shown in blue. Proteins that were significantly enriched, both in Drep-2^{GFP} flies and in independent control experiments with wild-type flies, are colored magenta (n = 35). Drep-2 and GFP are shown as green dots. (**C**) Classification of the 35 core network proteins; multiple counts were allowed. (**D**) Network of the 35 proteins that were significantly and reproducibly enriched in GFP pulldown experiments (at an FDR of 1%, magenta-colored dots in **B**). Additional putative interactors of the core network (FDR set at 10%) are shown in white (***Supplementary file 2***). The circle (node) and font size correspond to the rank within the results (indicated in ***Supplementary files 1 and 2***). The line (edge) width and shade correspond to the number of interactions each of the significantly enriched proteins has with others. The line/edge length is arbitrary. (**E**) Anti-FMRP probing confirmed the specific presence of FMRP in Drep-2^{GFP} complexes. Head extracts of flies expressing Drep-2^{GFP} or the presynaptic protein Syd-1^{GFP} were processed in parallel. FMRP was only enriched in preparations of Drep-2^{GFP} extracts. Immunoprecipitations were performed using either GFP-Trap-A beads (lanes labeled *IP*) or blocked agarose beads as binding control (labeled *Blank beads*).

DOI: 10.7554/eLife.03895.013

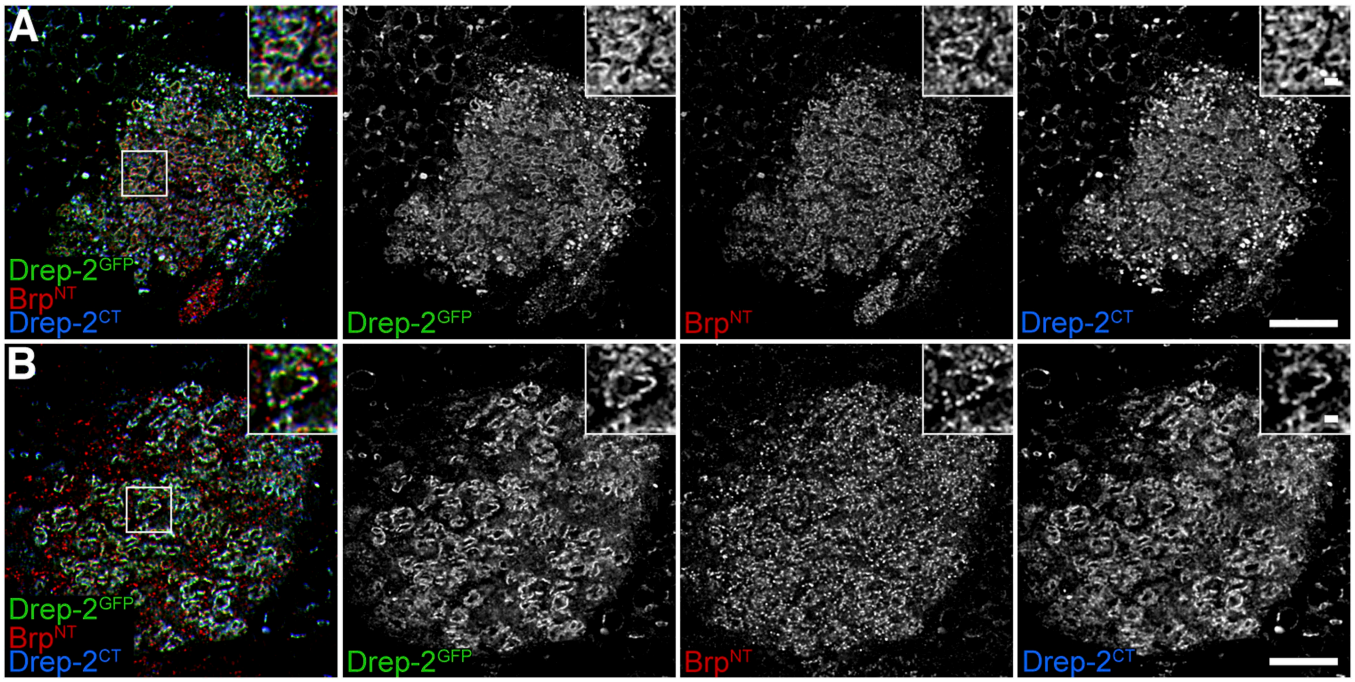

Figure 7—figure supplement 1. Drep-2^{GFP} colocalizes with endogenous Drep-2. (**A**) Pan-neural overexpression of UAS-drep-2^{GFP} by elav^{c155}-Gal4. MB calyx stained with anti-GFP, Brp$^{N\text{-}Term}$ and Drep-2$^{C\text{-}Term}$. The Drep-2^{GFP} label does not differ from the Drep-2$^{C\text{-}Term}$ antibody staining, compare also to ***Figure 4*** and ***Figure 4—figure supplement 1***. Scale bars: 10 μm and 1 μm (insets). (**B**) KC-specific expression of UAS-drep-2^{GFP} by mb247-Gal4 in *drep-2*^{ex13} mutants. Staining and scale bars as in (**A**).

DOI: 10.7554/eLife.03895.014